Journal of Mines, Metals and Fuels, *73(2): 377-384; 2025. DOI: 10.18311/jmmf/2025/47396*

Print ISSN : 0022-2755

Journal of Mines, Metals and Fuels

Contents available at: *www.informaticsjournals.co.in/index.php/jmmf*

Comparative Study of Helical Coil, Spiral Coil and Conical Coil (90^{O}) Heat Exchanger for Single Phase Fluid Flow

Pramod Purandare[1], Rahul Shivaji Yadav[1]*, Anurag Ashokkumar Nema[2], Atul Kulkarni[3], Swanand Kirpekar[1], Barister Giri[4], Prashant Ashok Patil[5], Manoj Jagdale[3] and Anant Sidhappa Kurhade[5]

[1]Department of Mechanical Engineering, Marathwada Mitramandal's College of Engineering Karvenagar - 411052, Maharashtra, India; yahulyadav491@gmail.com

[2]Department of Mechanical Engineering, School of Engineering and Sciences, MIT Art Design and Technology University, Loni Kalbhor, Pune - 412201, Maharashtra, India

[3]Department of Mechanical Engineering, Vishwakarma Institute of Information Technology, Kondhwa bk - 411048, Maharashtra, India

[4]Department of Mechanical Engineering, Rajgad Dnyanpeeth Technical Campus Polytechnic, Dhangawadi, Pune - 412205, Maharashtra, India

[5]Department of Mechanical Engineering, Dr. D. Y. Patil Institute of Technology, Pimpri - 411018, Pune, Maharashtra, India

Abstract

In the present study experimental analysis of the helical, spiral and conical coil with cone angle 90O for single-phase fluid flow is reported. Three different coil configurations are analysed under steady-state conditions. These three different coils (helical, spiral and conical coils) are formed with the same average coil diameter, tube diameter and tube length. For the analysis, an experimental setup with suitable instrumentation is developed. For each coil, sufficient numbers of test runs are conducted and readings are recorded with constant inlet temperature of cold and hot fluids as well as constant flow rate in every test run, to ensure the steady state. From the recorded results of the experimentation, heat transfer coefficients are calculated and the calculations are extended to calculate the Nusselt number (Nu) and effectiveness. The comparison of the results is presented from the analysis. Furthermore, the analysis is extended to predict the outlet temperature of hot and cold fluid, which shows good agreement with the experimental values.

Major Findings: *The helical coil exhibited the highest Nusselt number (Nu), while the spiral coil had the lowest Nu. The conical coil demonstrated intermediate Nu values. The effectiveness (ε) of the coiled tube heat exchanger is inversely proportional to the parameter Z. Consequently, the effectiveness of the system can be readily predicted using graphical patterns.*

Keywords: *Curved Tubes, Effectiveness, Heat Exchanger, Heat Transfer Coefficient, Thermal Analysis*

**Author for correspondence*

1.0 Introduction

1.1 Origin of Study

A heat exchanger is a vital component in the process industry, commonly used to transfer thermal energy between fluids. An optimized design of a heat exchanger aims to maximize heat transfer efficiency while minimizing pressure drop simultaneously[1]. The key factor in improving heat transfer performance is the heat transfer coefficient. However, increasing this coefficient typically results in a higher pressure drop across the exchanger. Therefore, selecting the ideal configuration is critical for achieving an optimal balance in heat exchanger design.

Heat transfer enhancement methods fall into two main categories: Active and Passive techniques. Active techniques rely on external forces to improve performance, such as fluid vibration, electric fields, and surface vibrations. On the other hand, passive techniques do not require external forces but instead focus on specialized surface designs, fluid additives, and tube inserts. Among the passive techniques, coiled tube configurations are particularly effective and widely utilized in industries. These systems offer numerous benefits, including higher heat transfer rates, compact design, self-cleaning properties, reduced fouling, modularity, and the elimination of costly expansion joints[2].

Several researchers have proved that coiled tubes are superior to straight tubes when employed in heat transfer applications[3,4]. When fluid flows through a curved tube, secondary flow patterns are generated due to the centrifugal forces acting on the fluid. This secondary flow creates turbulence within the coil, disrupting the laminar boundary layers and promoting a more chaotic fluid movement. The increased turbulence enhances the heat transfer rate by improving fluid mixing, which accelerates thermal exchange between the fluid and the tube surface. This phenomenon is particularly beneficial in the laminar flow regime, where heat transfer is typically lower due to the smooth and predictable flow patterns. The turbulence induced in curved tubes helps overcome this limitation, boosting heat transfer efficiency. Thermal performance and pressure drop of a shell and helically coiled tube heat exchanger with and without helical crimped fins have been investigated by Naphon[5]. Naphon and Wongwises[6] provided a literature review on heat transfer and flow characteristics of single-phase and



Figure 2. Spiral, helical and conical coils for heat exchanger.

two-phase flow in curved tubes including helically coiled tubes and spirally coiled tubes[7-10]. Some authors[11-14] focus on cone-shaped helical heat exchangers with varying coil angles, specifically 80°, 70°, and 60°. However, they do not provide a comparative analysis of helical, spiral, and conical coils at 90° for single-phase fluid flow. The performance of conical helical coil heat exchangers is studied using Computational Fluid Dynamics (CFD). In this study, the author used two shell geometries: a straight shell and a conical shell[15].

Shital *et al.*[16] provided critical reviews on heat transfer enhancement in heat exchangers. Khot Rahul and colleagues[17-21] studied the impact of laser welding parameters on the strength of TRIP steel. Anant *et al.*[22-25] focused on numerical thermal control of IC chips. Patil *et al.*[26] have discussed the Gadekar[27] MQL applications in grinding and lubrications while Yadav *et al.*[28-33] discussed different engineering applications.

The Conical Coiled Configuration (CCC) combines elements of both helical and spirally coiled designs, offering enhanced performance over each individual. This hybrid structure incorporates the advantages of both configurations, such as improved heat transfers and reduced pressure drop. The CCC's design allows for a more efficient fluid flow pattern, further optimizing heat exchange. As shown in Figure 1, the photographic presentation compares the distinct shapes of helical, spiral, and conical coils, illustrating their structural differences. The conical coiled configuration combines the benefits of both helical and spiral coil designs, enhancing heat transfer performance while minimizing pressure drop. A review of the literature shows that substantial experimental and numerical data exist for the analysis of helical and spiral-coiled heat exchangers. However, limited data is available

for conical coil heat exchangers. This study aims to fill this gap by conducting a comparative thermal analysis of all three coil types—helical, spiral, and conical—under identical geometric and operating conditions, providing valuable insights into their relative performance in heat exchange applications.

2.0 Experimental Setup

The coils are developed from the copper tube of 10X12mm (IDXOD). The length of the tube considered is 3m for each coil so that the heat transfer area for all coils remains the same. The average coil diameter of a helical coil is considered the pitch diameter of the coil whereas for conical and spiral coil it is the average of minimum and maximum diameter.

2.1 Dimensions Considered for the Analysis

The average diameter considered for the coil is 200 mm. The curvature ratio (δ) is the ratio of the diameter of the tube to the average diameter of the coil hence it is 0.05. The coil height is different for all three configurations. The average number of turns we are observing for all three coils is 4.5 to 5. Details of the coils are as per Table 1.

Helical, spiral and conical coils are precisely developed on the wooden former. For the proper dimensions of the coil, three different formers (one for each) are developed from wooden material. At the time of coil winding, tubes are filled with fine-grade sand to avoid deformation and pitching of the tube as well as to have precise dimensions and to maintain proper inside surface finish and dimensions. To avoid spring-back action in the copper tube material, bending is done by heating the coiled tubes. Hence the dimensions are tightly maintained.

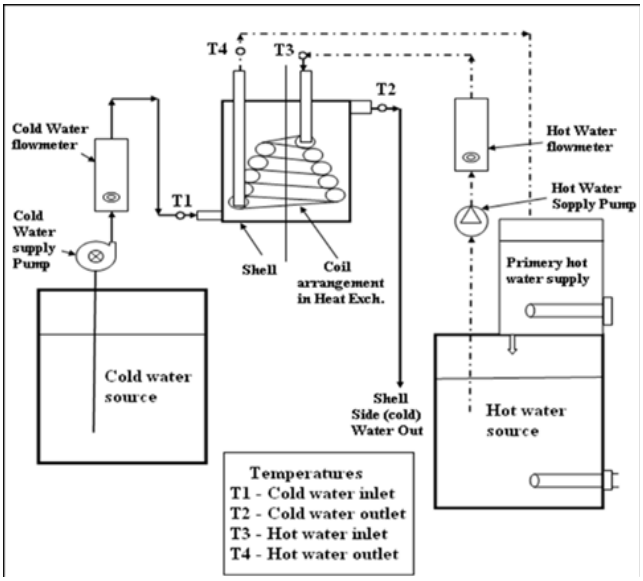


Figure 2. Experimental setup.

The experimental setup used for the analysis of the coiled heat exchanger is shown in Figure 2. It consists of a heat exchanger that houses multiple coils, each positioned within the same shell. Cold water is supplied to the shell side by a pump connected to a sufficiently large cold water storage tank, ensuring a constant inlet temperature. A specially designed constant temperature hot water supply system delivers hot water to the tube side of the heat exchanger via a separate pump. The hot water exits the heat exchanger and returns to the hot water supply tank. To measure the flow rates of both cold and hot water through the heat exchanger, the setup is equipped with two high-accuracy Rotameters, which offer a precision of 0.1% at maximum flow conditions. These flow meters enable precise monitoring of the water flow rates, essential for accurate performance analysis of the heat exchanger.

Table 1. Characteristic dimensions of shell and coil heat exchanger

Coil type	Min dia (mm)	Max dia (mm)	Pitch of coil (mm)	Dm (mm)	Length of tube m.
Helical Coil	194	206	13	200	3
Conical Coil with cone angle 90^{O}	180	220	13	200	3
Spiral Coil	165	235	13	200	3

Care has been taken to maintain the constant inlet temperatures of cold and hot water flowing through the heat exchanger during the experimentation. To minimize heat loss from convection, both the heat exchanger and

Table 2. Parameters considered for the conical coil analysis

S. No	Parameter	Details
1	Tube I.D.X O.D.	10X12mm
2	Coil Mean Diameter	200mm
3	Tube side fluid	Hot water of temperature 70 deg ±2%
4	Shell side fluid	Cold water of temperature 26 deg ±1%
5	Hot water flow rate (LPH)	10 lph to 100 lph (interval of 2.5 lph)
6	Cold water flow rate	30 lph to 90 lph (interval of 15 lph)

Associated pipelines are fully insulated using a suitable insulating material, such as silicon rope. This ensures that no heat is lost from the outer surface, enhancing the system's efficiency. Temperature measurements are taken at the inlet and outlet of both the cold and hot water streams using K-type thermocouples, with an accuracy of 0.1°C. Fluid properties are calculated at the mean temperature, determined as the average of the inlet and outlet temperatures for both the tube and shell side fluids.

2.2 The Parameters Considered for the Analysis

For the experimentation and the analysis of the conical coil heat exchanger the parameters considered are listed in Table 2.

3.0 Experimental Setup

The experimental parameters outlined in Table 1 indicate a broad range of flow rates were tested for both the tube and shell sides of the heat exchanger. The experiments were conducted for three types of coil configurations: helical, conical, and spiral. This comprehensive testing process involved a total of 125 test runs for each coil type, ensuring a thorough analysis of their performance under various flow conditions. The wide range of flow rates allowed for a detailed comparison of the heat transfer characteristics for all three coil configurations. Heat transfer to the cold water in the heat exchanger, Q_c, is calculated by the equation;

$$Q_c = m_c * C_{pw} * (t_{c,o} - t_{c,i}) \quad (1)$$

Where m_c represents the mass flow rate of cold water, C_{pw} is the specific heat capacity of water, and $t_{c,i}$ and $t_{c,o}$ are the inlet and outlet temperatures of the cold water, respectively. These parameters are crucial for determining the thermal performance of the heat exchanger, enabling accurate calculations of heat transfer rates and system efficiency. Heat transfer to the hot water in the heat exchanger, Q_h, is calculated by the equation;

$$Q_h = m_h * C_{pw} * (t_{h,o} - t_{h,i}) \quad (2)$$

where m_h is the mass flow rate of cold water, C_{pw} is the specific heat of the water and $t_{h,i}$ and $t_{h,o}$ are the temperatures of cold water at the inlet and outlet respectively. The average heat transfer rate, Q_{avg}, used in the calculation is determined from the hot water-side and cold waterside as;

$$Q_{avg} = \frac{Q_c + Q_h}{2} \quad (3)$$

The overall heat transfer coefficient, U_o was calculated from the temperature's inlet and outlet temperatures as;

$$U_i = \frac{Q_{avg}}{A_i * LMTD} \quad (4)$$

where, A_i, is the outside heat transfer surface area of the tube, Q is the heat transfer rate, whereas $LMTD$ is the log mean temperature difference. The calculation of $LMTD$ is considered as per the coulter flow condition[7];

$$LMTD = \frac{\Delta T_1 - \Delta T_2}{\ln(\frac{\Delta T_1}{\Delta T_2})} \quad (5)$$

Where ΔT_1 is the temperature difference between the inlet temperature of hot water and the outlet temperature of cold water and ΔT_2 is the temperature difference between the outlet temperature of hot water and the inlet temperature of cold water.

The heat transfer coefficients for the tube-side h_i and shell-side h_o were determined using the Wilson plot method[8]. Wilson plots provide a systematic approach for calculating individual heat transfer coefficients based on the overall heat transfer coefficient. This method involves plotting the reciprocal of the heat transfer rate against the reciprocal of the temperature difference, allowing for the calculation of both the tube-side and shell-side heat transfer coefficients. The overall heat transfer coefficient (UUU) is related to the inner and outer heat transfer coefficients through the following equation;

$$\frac{1}{U_i} = \frac{A_{oi}}{A_0 h_0} + \frac{A_i ln\left({}^{d_o}/_{d_i}\right)}{2\pi kL} + \frac{1}{h_i} \qquad (6)$$

In this context, d_o and d_i represent the outer and inner diameters of the tube, respectively, k is the thermal conductivity of the tube material, and L is the length of the tube within the heat exchanger. One of the advantages of this method is that it eliminates the need to measure the tube wall temperature, preventing any disturbances in the flow patterns or heat transfer caused by temperature measurements. Wilson plots are constructed by determining the overall heat transfer coefficients across several trials, with one fluid flow kept constant while the other is varied. In this study, the shell-side flow was maintained constant, while the tube-side flow rate was adjusted for different conditions, allowing for a detailed evaluation of heat transfer performance under varying flow rates. It is assumed that as the flow rate of the shell side is kept the same the thermal resistance of the shell side may remain constant. The inner heat transfer coefficient is assumed to behave in the following manner with the fluid velocity in the shell, v_i;

$$h_i = C * {v_i}^n \qquad (7)$$

The values of constant, C, and the exponent n were calculated by substituting Equation (7) into Equation (6) and then evaluating the same by curve fitting. From this, the heat transfer coefficient inside the tube, hi and outside the tube ho are calculated and from these values, the values of Nui and Nuo are estimated. The effectiveness (Є) of the heat exchangers[9] is calculated by calculating the heat capacity of the hot and cold fluids (Ch and Cc respectively) flowing through the heat exchanger and by using the correlation;

$$Effectiveness, (\epsilon) = \frac{C_h * \left(t_{h,i} - t_{h,0}\right)}{C_{min} * \left(t_{h,i} - t_{c,i}\right)} = \frac{C_c * \left(t_{c,o} - t_{c,i}\right)}{C_{min} * \left(t_{h,i} - t_{c,i}\right)} \qquad (8)$$

The maximum heat capacity between hot and cold fluid heat capacities. The analysis is carried out by considering all the parameters related to heat exchanger.0020

4.0 Results and Discussion

To conduct a comparative thermal analysis of helical, spiral, and conical coils with a cone angle of 90°, three different coil configurations were tested under identical conditions. The coils shared the same geometric parameters, including the inner and outer diameters of the tube di and do and the mean coil diameter (DD), ensuring a fair comparison. Additionally, the experiments were carried out under the same operating parameters, with consistent flow rates for both shell-side ms and tube-side mw fluids, as well as constant inlet temperatures for both the hot thi and cold TC fluids. This setup allowed for an accurate evaluation of the thermal performance of each coil configuration. Figure 3 shows the variation of Nu concerning Re for the different coils.

The analysis reveals that the Nu value decreases from helical to conical and further to spiral for the same Re. It is also observed that the variation in Nu is sufficiently high at low Re, whereas it goes on reducing as the Re value goes on reducing. Hence, it may be concluded that the secondary flow effect is more effective at lower Re

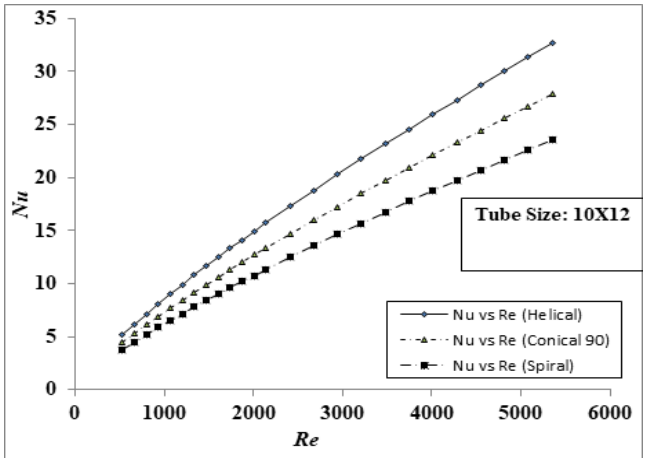


Figure 3. Variation of Nu concerning Re for different coils.

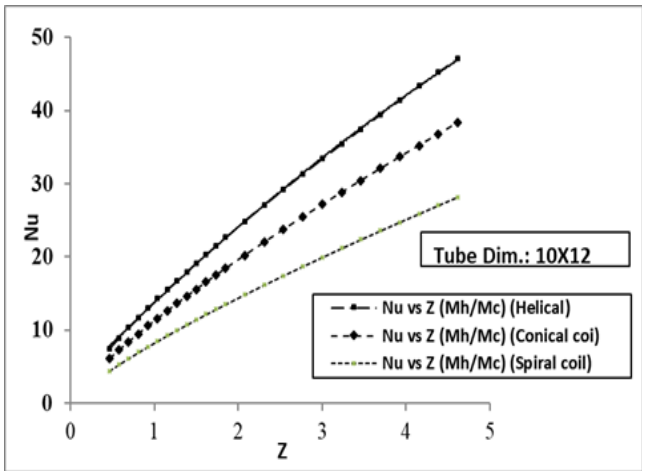


Figure 4. VVariation of Nu concerning Z for different coils.

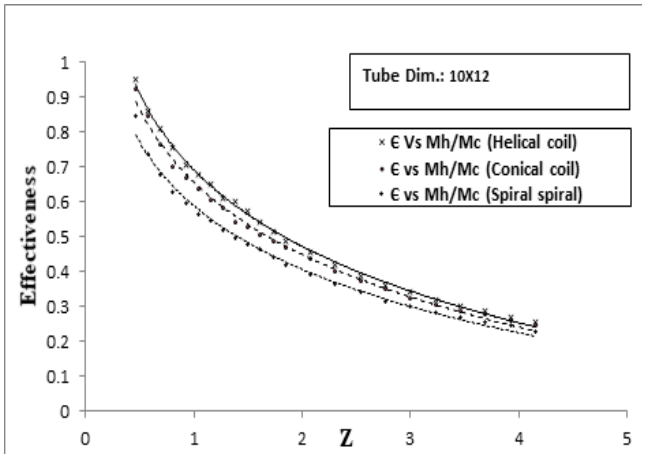


Figure 5. Variation of Effectiveness (Є) concerning Z for different coils.

than at high Re numbers. Figure 4 shows that there is a direct relationship between the Nusselt number, Nu, and the parameter Z; this means that the Nusselt number is dependent on the mass flow rate of both fluids. An increase in the mass flow rate in hot fluid, m_h, causes an increase in the Nusselt number, thereby enhancing heat transfer. Conversely, when the mass flow rate of cold water m_c increases, it causes a decrease in the value of the Nusselt number. Figure 4 shows that there is a direct relationship between the Nusselt number, Nu, and the parameter Z; this means that the Nusselt number is dependent on the mass flow rate of both fluids. An increase in the mass flow rate in hot fluid, m_h, causes an increase in the Nusselt number, thereby enhancing heat transfer.

Looking at the figure in more detail, it can be realized that the helical coil configuration results in the highest effectiveness between the three different coil types analyzed. The spiral coil was shown to have the lowest effectiveness, while the conical coil falls in between with an effectiveness value that is higher than the spiral but lower than the helical one. This trend points out that the helical coil has a better performance in terms of heat exchange efficiency regardless of the condition of Z.

From Figure 5, it is clear that an increase in the parameter Z causes the heat exchanger's effectiveness to decrease. The graph has indicated that the sensitivity of the effectiveness is higher at the values of lower Z, as the slope of the curve becomes more pronounced. This implies that with lower values of Z, the different configurations of the coils are offered a higher efficiency. However, as Z increases, the slope of the graph flattens, meaning that a change in flow condition causes less change in performance due to coil configurations. Looking at the figure in more detail, it can be realized that the helical coil configuration results in the highest effectiveness between the three different coil types analyzed. The spiral coil was shown to have the lowest effectiveness, while the conical coil falls in between with an effectiveness value that is higher than the spiral but lower than the helical one. This trend points out that the helical coil has a better performance in terms of heat exchange efficiency regardless of the condition of Z.

5.0 Conclusion

This study provides a comprehensive comparative analysis of the heat transfer performance of helical, spiral, and conical coil heat exchangers. Three distinct heat exchangers, each with the same average coil diameter and tube length, were tested under identical operating conditions. The analysis revealed the following key findings:

- As hot water flow inside the tube increases, by keeping cold water flow outside the tube (shell side) constant, the tube side Nu increases. The helical coil has a maximum Nu whereas the spiral coil has minimum Nu and the conical coil has intermediate values of Nu. For the same Re helical coil shows higher Nu than the conical coil

and the conical coil has higher than the spiral coil configuration in the heat exchanger.

- For an increase in Z, the value of Nu increases. The helical coil has a maximum Nu whereas the spiral coil has minimum Nu and the conical coil has intermediate values of Nu. The effectiveness (Є) of the coiled tube heat exchanger is dependent on the parameter Z and decreases as Z increases. Among the coil configurations, the helical coil exhibits the highest effectiveness. From the effectiveness, we can easily predict the outlet temperatures of the hot and cold fluids as discussed.

6. 0 References

1. Patil RK, Shende BW, Ghosh PK. Designing a helical-coil heat exchanger. Chem Eng. 1982; 92(24):85-88.
2. Lines J. Helically coiled heat exchangers offer advantages. Bulletin HHE-30, Graham Manufacturing Co. Inc.
3. Prabhanjan DG, Raghavan GSV, Rennie TJ. Comparison of heat transfer rates between a straight tube heat exchanger and a helically coiled heat exchanger. Int Commun Heat Mass Transf. 2002; 29(2):185-191. https://doi.org/10.1016/S0735-1933(02)00309-3
4. Salimpour MR. Heat transfer characteristics of a temperature-dependent-property fluid in shell and coiled tube heat exchangers. Int Commun Heat Mass Transf. 2008; 35:1190-1195. https://doi.org/10.1016/j.icheatmasstransfer.2008.07.002
5. Naphon P. Study on the heat transfer and flow characteristics in a spiral-coil tube. Int J Heat Mass Transf. 2011; 38:69-74. https://doi.org/10.1016/j.icheatmasstransfer.2010.10.007
6. Naphon P, Wongwises S. Heat transfer coefficients under dry-and-wet surface conditions for a spirally coiled finned tube heat exchanger. Int Commun Heat Mass Transf. 2005; 32:371-385. https://doi.org/10.1016/j.icheatmasstransfer.2004.04.031
7. Ghorbani N, Taherian H, Gorji M, Mirgolbabaei H. An experimental study of thermal performance of shell-and-coil heat exchangers. Int Commun Heat Mass Transf. 2010; In press. https://doi.org/10.1016/j.icheatmasstransfer.2010.02.001
8. Shokouhmand H, Salimpour MR, Akhavan-Behabadi MA. Experimental investigation of shell and coiled tube heat exchangers using Wilson plots. Int Commun Heat Mass Transf. 2008; 35:84-92. https://doi.org/10.1016/j.icheatmasstransfer.2007.06.001
9. Ozisic MN. Heat Transfer—A Basic Approach. New York: McGraw Hill; 1985.
10. Dravid AN, Smith KA, Merrill EW, Brian PLT. Effect of secondary fluid motion on laminar flow heat transfer in helically coiled tubes. AIChE J. 1971; 17(5):1114-1122. https://doi.org/10.1002/aic.690170517
11. Bhirdi VD, Mane NS, Patil AM. Experimental investigation of heat transfer through a cone-shaped helical heat exchanger with varying coil angle. In: Pawar P, Ronge B, Balasubramaniam R, Vibhute A, Apte S, editors. Techno-Societal 2018. Cham: Springer; 2020. https://doi.org/10.1007/978-3-030-16962-6_43
12. Pawar SS, *et al.* A critical review of heat transfers through helical coils of circular cross-section. J Sci Ind Res. 2011; 70:835-843.
13. Abo Elazm M, Ragheb A, Elsafty A, Teamah M. Computational analysis for the effect of the taper angle and helical pitch on the heat transfer characteristics of the helical cone coils. Arch Mech Eng. 2012; 59(3):1-9. https://doi.org/10.2478/v10180-012-0019-9
14. Shinde DD, Dange HM. Heat transfer analysis of a cone-shaped helical coil heat exchanger. Int J Innov Eng Technol. 2013; 3(1):1-6.
15. Kumar A, Pandey V. CFD analysis of shell and coil heat exchanger by using different mass flow rates for hot and cold fluid. Int J Res Appl Sci Eng Technol. 2022; 10(11):1592-1608. https://doi.org/10.22214/ijraset.2022.47683
16. Waware SY, Chougule SM, Yadav RS, *et al.* A comprehensive evaluation of recent studies investigating nanofluids utilization in heat exchangers. J Adv Res Fluid Mech Therm Sci. 2024; 119(2):160-172. https://doi.org/10.37934/arfmts.119.2.160172
17. Khot RS, Kadam PR. Structural behaviour of fillet weld joint for bimetallic curved plate using Finite Element Analysis (FEA). In: 6th International Conference on Advanced Research in Arts, Science, Engineering and Technology (ICARASET); 2021; 23-8.
18. Khot RS, Rao TV. Investigation of mechanical behaviour of laser welded butt joint of Transformed Induced Plasticity (TRIP) steel with effect of laser incident angle. Int J Eng Res Technol. 2020; 13(1):3398-3403. https://doi.org/10.37624/IJERT/13.11.2020.3398-3403
19. Khot RS, Rao TV, Harshad N, *et al.* An investigation on laser welding parameters on the strength of TRIP steel. Stroj Vestn/J Mech Eng. 2021; 67(1-2):45-52. https://doi.org/10.5545/sv-jme.2020.6912
20. RS, Rao TV. Effect of quenching media on laser butt welded joint on Transformed-Induced Plasticity (TRIP)

steel. Int J Emerg Trends Eng Res. 2020; 8(10):7686-7691. https://doi.org/10.30534/ijeter/2020/1588102020
21. Khot RS, Rao TV, Keskar A, *et al.* Investigation on the effect of power and velocity of laser beam welding on the butt weld joint on TRIP steel. J Laser Appl. 2020; 32(1):012016. https://doi.org/10.2351/1.5133158
22. Kurhade AS, Waware SY, Bhambare PS, *et al.* A comprehensive study on *Calophyllum inophyllum* biodiesel and dimethyl carbonate blends: Performance optimization and emission control in diesel engines. J Mines Met Fuels. 2024; 72(5):499-507. https://doi.org/10.18311/jmmf/2024/45188
23. Kurhade AS, Biradar R, Yadav S, Patil P, Kardekar NB, Waware SY, *et al.* Predictive placement of IC chips using ANN-GA approach for efficient thermal cooling. J Adv Res Fluid Mech Therm Sci. 2024; 118(2):137-147. https://doi.org/10.37934/arfmts.118.2.13714717
24. Kurhade AS, Waware SY, Munde KH, *et al.* Performance of solar collector using recycled aluminium cans for drying. J Mines Met Fuels. 2024; 72(5):455-461. https://doi.org/10.18311/jmmf/2024/44643
25. Patil P, Kardekar N, Yadav R, *et al.* Al2O3 nanofluids: An experimental study for MQL grinding. J Mines Met Fuels. 2023; 2751-2756. https://doi.org/10.18311/jmmf/2023/41766
26. Gadekar TD, Kamble DN, Ambhore NH. Experimental study on gear EP lubricant mixed with $Al_2O_3/SiO_2/ZrO_2$ composite additives to design a predictive system. Tribol Ind. 2023; 45(4):579-590. https://doi.org/10.24874/ti.1461.03.23.07
27. Yadav R. Experimental and numerical study of welded curved plates. Int J Innov Eng Res Technol. 2019; 6(2):1-7.
28. Yadav R, Potdar M, Kanwade A, *et al.* Design and development of BIW (Body in White) fixture for tunnel panel with robotics simulation. Indian J Tech Educ. 2024; 47(1):112-116.
29. Yadav RK. FEA-based validation of weld joint used in chassis of Light Commercial Vehicles (LCV) in tensile and shear conditions. Int J Innov Eng Res Technol. 2015; 2(3):1-7.
30. Yadav RS, Gadekar T, Gundage V, *et al.* Numerical and experimental investigation of the effect of overlapping angle on strength and deformation of curved plate joined using an arc welding process. J Mines Met Fuels. 2024; 72(10):1059-1066. https://doi.org/10.18311/jmmf/2024/45697
31. Suryawanshi AM, Deshmukh PD, Lohate AK, *et al.* Dynamic performance evaluation of a five-phase induction motor system controlled using fuzzy logic director. J Mines Met Fuels. 2024; 72(9):915-922. https://doi.org/10.18311/jmmf/2024/45570
32. Yadav RS, Nimbalkar A, Gadekar T, *et al.* Comparison of experimental and numerical investigation of mono-composite and metal leaf spring. J Mines Met Fuels. 2024; 72(8):815-827. https://doi.org/10.18311/jmmf/2024/45325

Abbreviations

Nomenclature

d	Tube Diameter, *m*
D	Coil Diameter, *m*
h	Heat Transfer Coefficient, W/m^2K
k	Thermal Conductivity, *W/mK*
L	Tube Length, *m*
r	Tube Radius, *m*
R	Radius of Curvature, *m*
v	Velocity of Water, *m/s*
Z	Mass Flow Ratio (M_h/M_c)
C	Heat Capacity of Hot Fluid, *kJ*
M	Mass of Water, *kg*
Nu	Nusselt Number
U	Overall Heat Transfer Coefficient, W/m^2K
Re	Reynolds Number
Pr	Prandtl Number
De	Dean Number
ϵ	Effectiveness
LMTD	Log Mean Temperature Difference
A_c	Cross Section Area of the Pipe, m^2

Subscripts

i	Inside Condition
o	Outside Condition
c	Cold Fluid
h	Hot Fluid

Greek Letters

ρ	Density, kg/m^3
μ	Viscosity, Ns/m^2
δ	Curvature Ratio, *r/R*